ELECTRON PARTITIONING IN CONTINUOUS *RHODOBACTER SPHAEROIDES* CULTURES

by

UGUR SOHMEN

A report submitted in partial fulfillment of the requirements for the degree of

MASTER OF SCIENCE

(Environmental Engineering)

at the

UNIVERSITY OF WISCONSIN – MADISON

May 2011

TABLE OF CONTENTS

CHAPTER 1 – INTRODUCTION

Today's global energy requirements are mostly dependent on fossil fuels, the utilization of which are causing global climate change as well as leading to the foreseeable depletion of these limited non-renewable energy sources (Jean-Baptiste, 2003). As a result of growing concern over environmental impacts and depletion of existing fossil fuels, the interest in developing renewable, sustainable ways of energy generation has greatly increased. Among the different renewable energy types, the so-called biofuels are one of the most promising and studied forms of energy generation. There is a growing trend towards employing modern technologies and efficient bioenergy conversion using a range of biofuels, which are becoming cost-wise competitive with fossil fuels (Demirbas, 2007). Some of these biologically based fuels which are considered or developed as renewable replacements for fossil fuels are ethanol, various next generation liquid transportation additives, or gases such as hydrogen (H_2) or methane (CH_4).

The reason for the selection of hydrogen as the model biofuel is that the amount of energy produced during hydrogen combustion is higher than that released by any other fuel on a mass basis, with a low heating value (LHV) 2.4, 2.8 and 4 times higher than that of methane, gasoline and coal, respectively. Furthermore, hydrogen has a major advantage as a fuel because of the absence of CO_2 emissions, as well as other pollutant emissions (thermal NO_x) if it is employed in low temperature fuel cells. This is especially important for the transportation sector, which is responsible for 18% consumption of primary energy worldwide (Marban, 2007).

Hydrogen can be produced by a number of processes, including electrolysis of water, thermocatalytic reformation of hydrogen-rich organic compounds, and biological processes. Currently hydrogen is produced, almost exclusively, by electrolysis of water or by steam reformation of methane, which involves fossil fuel consumption for hydrogen production, thereby minimizing the energy benefits of this technology. Biological production of hydrogen (bio-hydrogen), using microorganisms, is an exciting

area of technology development that offers potential production of usable hydrogen from a variety of renewable resources. Biological systems provide a wide range of approaches to generate hydrogen, and include direct biophotolysis, indirect biophotolysis, photo-fermentations, and dark fermentations (Levin, 2004).

Among these systems, photo-fermentation is especially advantageous because photosynthetic bacteria can provide significant biologically-derived hydrogen as several species are able to generate large amounts of this fuel using energy from sunlight and renewable nutrients. More specifically, photoheterotrophic bacteria, which have the ability to simultaneously use energy derived from light and organic compounds to drive H_2 production, can be used to develop solar-driven biofuel production processes for the utilization of renewable organic substrates in a biofuel economy (Kapdan, 2006).

The objective of this work was to study the electron partitioning of the photosynthetic purple non-sulfur bacterium, *Rhodobacter sphaeroides*, under different environmental conditions (i.e., different growth rates). Quantifying the contribution of networks that impact solar powered hydrogen production can then be used for the development of a genome-scale metabolic network model of *R. sphaeroides* (Saheed et al, submitted). Previous research investigated the electron partitioning in batch cultures of *R. sphaeroides* (Yilmaz et al., 2010). However, for the purpose of metabolic model development, quantitative analysis of electron partitioning is needed on continuous steady-state *R. sphaeroides* cultures. The establishment and design of the metabolic model will increase the feasibility of using bio-hydrogen as an alternative fuel and will provide insights for practical applications in the future.

CHAPTER 2 – BACKGROUND

2.1 Electron Fate Distribution in Photoheterotrophic Batch *Rhodobacter sphaeroides* Cultures

The partitioning of reducing power into different electron-accepting pathways during different growth stages of H_2 producing *R. sphaeroides* cultures was recently studied (Yilmaz et al., 2010). The method developed by Yilmaz et al. (2010) is used here for evaluating the partitioning of electrons in continuous *R. sphaeroides* cultures. This chapter summarizes the previously developed electron balance method for quantitatively analyzing the partitioning of nutrient electrons by the chemical oxygen demand (COD) concept. The approach is based on the theoretical or experimental assessment of the COD of products from different electron-accepting reactions (Figure 2.1). Briefly, the COD of the electron accepting products should be equal to the COD of the substrate (carbon source plus the nitrogen source). In batch cultures, the four electron sinks (cells, PHB, H_2 and SMP) shown in Figure 2.1 accounted for greater than 85% of the electrons provided by the nutrients, indicating a fairly good overall electron balance (Yilmaz et al. 2010).

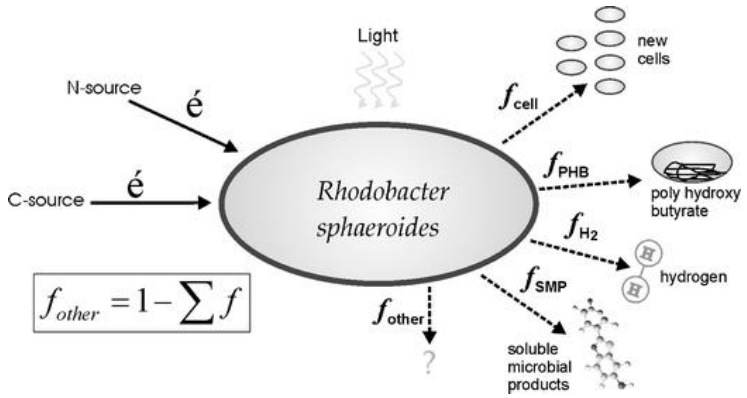

Figure 2.1 Electron fate model of *R. sphaeroides*. Fraction of substate electrons is designated by ***f***.

As mentioned earlier, COD was used to quantify electron availability and partitioning in gaseous, soluble, and particulate electron sinks. Theoretical COD values of substrates and H_2 were calculated using the following equation (Rittmann, 2001):

$$C_nH_aO_bN_c + \left(\frac{2n + 0.5a - 1.5c - b}{2}\right) O_2 \rightarrow nCO_2 + cNH_3 + \frac{a - 3c}{2}H_2O$$

The stoichiometry in this reaction defines the theoretical oxygen demand for the full oxidation of an organic compound to CO_2. For instance, the moles of O_2 required for the complete oxidation of 1 mmol of succinic acid ($C_4H_6O_4$) can be calculated to be equal to 3.5 mmol of O_2. Since the molecular weight of O_2 is 32 mg/mmol, the theoretical COD of succinic acid is 112 mg COD per milimole. In this way, the concentrations of the carbon and nitrogen sources in the media as the initial electron donors and the amount utilized by the bacteria are converted to COD units. Hydrogen gas production was also converted to COD units using the same formula and the theoretical COD for H_2 is 16 mg COD per milimole of H_2. For mixed and unknown organic material, the COD cannot be calculated from the above equation but can be obtained experimentally (as described in Chapter 4). Finally, when all the compounds have the same common unit as mg COD/L, the mass balance can be established and analyzed for the role and influence of different competing metabolic pathways for biofuel production.

Yilmaz et al. (2010) used sets of batch cultures incubated with different carbon sources and analyzed electron partitioning in terms of COD at different growth stages of *R. sphaeroides*. As an example, the COD distribution of a lactate-fed culture is shown in Figure 2.2. At each of the sampled points, the concentrations of extracellular carbon and nitrogen sources were measured and converted to COD to quantify the reducing power remaining and consumed at different stages of growth. The COD on the y-axis in Figure 2.2 corresponds to the amount of COD utilized from the carbon and nitrogen sources. The difference between the measured soluble COD in the media and the COD from the remaining carbon

and nitrogen sources corresponded to the Soluble Microbial Products (SMP) accumulation. The COD sum of the end products is compared to the total substrate COD utilized (i.e., carbon and nitrogen sources consumed) and the difference indicated as COD_{other} in Figure 2.2, which represents potentially unaccounted electron sinks or the accumulation of experimental error from individual products. As can be seen from Figure 2.2, the cumulative amount of electrons directed toward H_2 production continuously increased, with 55% of the total produced during growth phase and the rest in the stationary phase. Cell synthesis and PHB were important electron sinks only during the growth phase, while the importance of (SMP) in the electron balance significantly increased in the stationary phase.

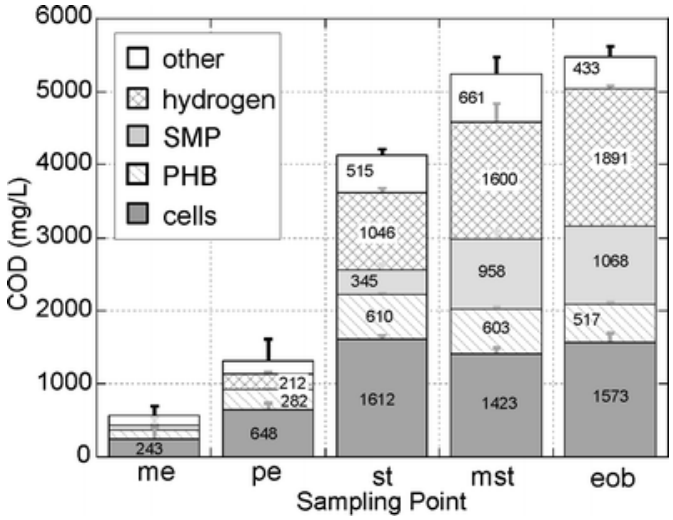

Figure 2.2 Time series of COD distribution in lactate-fed batch cultures. me=mid-exponential point, pe=post-exponential phase, st=beginning of stationary phase, mst=mid-stationary phase, eob=end of batch. Source: Yilmaz et al. (2010).

The data from the distribution of reducing power for different phases of growth as well as for the mutants of *R. sphaeroides* were useful to inform genome-scale metabolic network models of *R. sphaeroides* that can provide predictions on the flow of reducing power needed to further improve the biofuel production (Yilmaz et al., 2010).

2.2 CHEMOSTAT THEORY

Continuous addition of fresh medium in order to prolong a culture of microbes for continuous harvesting of products has been discussed for more than half a century. Among these continuous systems, a chemostat is advantageous over a plug-flow culture because the plug-flow system simulates a batch culture and does not offer any means of environmental control not applicable in a batch culture (Pirt, 1975). The fundamental importance of chemostat cultures became apparent after the formulation of the basic theory by Monod (1950). The theory first indicated that it should be possible to fix the specific growth rate of the biomass at any value from zero to maximum, which broke a barrier in traditional thinking that implicitly assumed that the only stable bacterial growth rate was the maximum rate corresponding to the doubling time in a simple batch culture (Pirt, 1975). Thus, chemostat cultures opened up new horizons in microbial physiology. Moreover, the history of how chemostats became useful tools in microbiology shows a prime example of the importance of theory development before experimentation. In this chapter, the general working principle of the chemostat, specific growth rate, distribution of residence times and finally deviations from the ideal conditions will be explained.

2.2.1 General Principle

A chemostat consists of a culture into which fresh medium is continuously introduced at a constant rate and the culture volume is kept constant by continuous removal of culture (Figure 2.3). Ideally the mixing should be perfect, that is a drop of medium entering the chemostat should instantly be distributed uniformly throughout the whole reactor. In practice this means that the time required to mix a small volume of medium with the culture should be small compared with the retention time (t_r) given by V/Q, where V is the reactor volume and Q is the medium flow rate (Pirt, 1975).

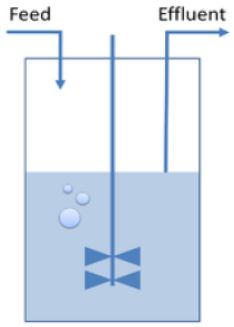

Figure 2.3 Chemostat Schematic

In a typical start-up of a chemostat reactor, the bacterial culture is allowed to grow as a batch (i.e., without the addition of medium) before starting the continuous flow of medium into the reactor (from time zero until time t_1 in Figure 2.4). After this point, there are three possible outcomes with respect to the biomass and substrate concentrations in the chemostat. These three possibilities are illustrated in Figure 2.4 (Pirt, 1975).

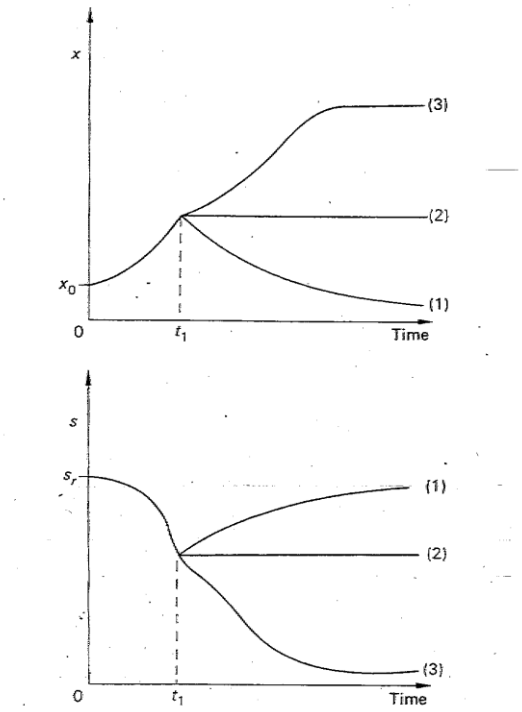

Figure 2.4 The three possible outcomes of a chemostat culture in which growth rate of the biomass (*X*) is limited by the concentration of the growth-limiting nutrient (*S*). Continuous flow of medium with a concentration of Substrate (S_r) is started at time t_1. (1) Wash-out conditions, (2) Steady-state conditions, (3) Increasing biomass conditions. Source: Pirt (1975).

The first possibility is that the rate of washout of biomass will exceed the rate of growth so that the biomass concentration will decrease and the growth-limiting substrate concentration will increase. With a higher substrate concentration, growth rates will increase, potentially reaching a steady state condition in which the rate of growth equals the washout rate. The second possibility is that the rate at which the biomass leaves the reactor will be exactly the same as the growth rate. In this case there will be an immediate steady state in which the biomass and the substrate concentrations remain constant. The third possibility would occur if the rate of biomass leaving the reactor were initially less than the growth rate. In this case the biomass concentration will continue to increase. However, eventually the decrease in the substrate concentration must decrease the specific growth rate until the biomass growth rate equals the rate of biomass leaving the reactor. Then there can be no further changes in the concentrations of biomass and the specific growth rate of the biomass is determined by the flow rate. This steady state is a self-regulating one, with the consequences of temporary disturbances of the steady-state conditions are depicted in Figure 2.5.

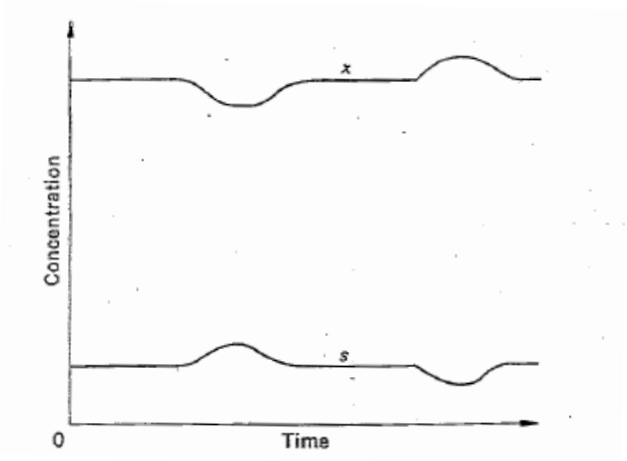

Figure 2.5 Effects of temporary disturbances when the specific growth rate is less than the maximum rate. A fall in the biomass concentration (*X*) will be associated with a rise in the substrate concentration (*S*); this will increase the growth rate and act as to restore the steady state conditions. A rise in the biomass concentration will have the opposite effect.

2.2.2 Specific Growth Rate

The objective of this study is to achieve different growth rates and biomass concentrations under different conditions so that the values obtained from the experiments can be used for the development of the metabolic model of *R. sphaeroides*. The increase in biomass is given by the biomass balance, that is

Net increase in biomass = growth – output

For an infinitely small time interval *dt*, the balance for the culture can be written as:

$$V \cdot dX = V \cdot \mu X \cdot dt - QX \cdot dt$$

where μ is the specific growth rate, *V* is the culture (reactor) volume, and *Q* is the flow rate. Dividing this equation by *V.dt*, the following equation is obtained:

$$\frac{dX}{dt} = (\mu - D) \cdot X$$

Where *D* is defined as the dilution rate, and is equal to *Q⁄V*. Hence at steady state, when *dX/dt* is zero, specific growth rate is equal to the dilution rate. By changing the flow rate of the medium, different dilution rates can be obtained and different growth rates can be achieved for analyzing the behavior of *R. sphaeroides* under a variety of conditions.

2.2.3 Distribution of Residence Times in a Chemostat

In a chemostat, through mixing, each element of medium added may emerge at once from the culture or remain in the culture. That is, there will be a distribution of residence times. If m_o is the amount of material per unit volume present at zero time and *m* is the amount present at time *t*, then the amount of material leaving the reactor or with residence time between *t* and *t + dt* will be

$$-dm = Dm \cdot dt \qquad (\text{where } D \text{ is the dilution rate})$$

If the fraction of the original material with residence time between t and $t + dt$ is defined as $dm/m_o = -df$, then the following equation is obtained:

$$df = D\frac{m}{m_o}\,dt$$

Since $-dm/dt = Dm$, it follows that $m/m_o = e^{-Dt}$, hence $df = De^{-Dt}\,dt$. The fraction of material with residence times between t_1 and t_2 will be:

$$F = \int_{t_1}^{t_2} De^{-Dt}\,dt$$

The function $De^{-Dt} = df/dt$ represents the distribution of residence times. Integration of this above equation gives:

$$F = e^{-Dt_1} - e^{-Dt_2}$$

Thus the fraction with residence time between 0 and t is $(1 - e^{-Dt})$ and it can be calculated that the fractions of the original material remaining after 1, 2, 3 and 4 replacement times (a.k.a. residence times) are 0.367, 0.135, 0.050 and 0.015, respectively as shown in Figure 2.6.

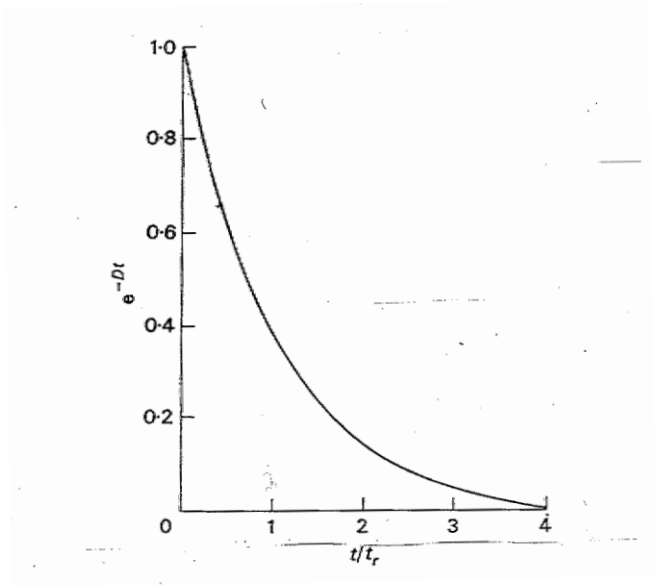

Figure 2.6 Fraction (e^{-Dt}) of initial material remaining in a chemostat after elapse of different multiples of the residence time, t_r (Pirt, 1975).

The distribution may also be determined experimentally by injecting a small volume of dye into the reactor and collecting the effluent in small fractions. The plot of the dye contents of the fractions against time gives the distribution of residence times. The exponential distribution of residence times obtained with the chemostat shows the practical importance of waiting at least 4 residence times in order for the initial medium to be cleared out with the new medium flowing in and makes it a safe bet for reaching the steady state conditions by allowing the reactor to have at least 4-5 residence times before assuming that the steady state conditions are achieved.

2.2.4 Deviations from the Ideal Reactor Behavior

Good mixing in a chemostat culture implies that the time taken for the material to become homogeneously dispersed throughout the reactor should be very small compared with the nominal residence time, which is defined as $t_d = 1/D$. However, perfect mixing may not be achieved in laboratory-scale reactors especially if the reactor has a design that prevents the complete mixing. If mixing is imperfect, there will be spaces in the reactor in which the dilution rates are either less or greater than the mean dilution rate (D) given by Q/V. This means that the dilution rates at various points in the vessel will be distributed about the mean, D. Consequently when D reaches a critical value D_c there will be some points in the reactor where $D < D_c$ and steady states can be obtained when $D > D_c$. Such a deviation from the theoretical behavior has been termed an 'apparatus effect' (Herbert, 1958).

Many microorganisms can adhere to glass and metal surfaces and in continuous-flow cultures of long duration there may be so-called wall growth which may vary from a light film of biomass to a massive accretion of it on the reactor surface. This wall growth can erroneously change the critical dilution rate since actual washout will not happen as the microorganisms are attached to the walls without any mixing. To maintain effectively homogeneous conditions in a chemostat culture, wall growth must be minimized by vigorous agitation.

CHAPTER 3 – EXPERIMENTAL SET-UP

In order to analyze the electron partitioning in continuous *R. sphaeroides* cultures, four chemostat reactors were set up and run until steady-state conditions were reached. The chemostat reactors were operated under anaerobic photosynthetic conditions and under aerobic dark conditions to investigate the electron fate in *R. sphaeroides* in these two different living environments. This chapter explains the details of the experimental set-up of these reactors, seed culture conditions, media preparation and sample collection. The samples were analyzed according to the procedures and analytical methods that are explained in Chapter 4. Table 3.1 tabulates the culture conditions investigated in this study. The first four experimental set had anaerobic photosynthetic conditions and the last one had aerobic dark conditions as mentioned in Table 3.1

Table 3.1 Summary of the experimental schedule in this study

	Carbon Source: Succinic Acid Nitrogen Source: Glutamic Acid	Carbon Source: Succinic Acid Nitrogen Source: Ammonia	Carbon Source: Glucose Nitrogen Source: Glutamic Acid	Carbon Source: Glutamic Acid Nitrogen Source: Glutamic Acid	Carbon Source: Succinic Acid Nitrogen Source: Ammonia
RETENTION TIMES (h)	8	8	10	10	7.1*
	10	10	12	12	8.7*
	12	12		16	9.3*
	16	16		24	9.5*

*aerobic

3.1 CHEMOSTAT REACTOR SET-UP

In order to prevent the shading of light in dense cultures, 20 mL Pyrex tubes were used as reactors. The reactors were seeded with 200 µL of pre-cultured wild type (WT) *R. sphaeroides* and operated in batch mode until sufficient cell growth was achieved (~150 Klett Units). Then, the reactors were switched to a flow-through condition. All reactors had a 19-mL working volume and a 1-mL headspace. The reactors were capped with rubber stoppers. Influent media was prepared in 300-mL flasks and pumped into each reactor using peristaltic pumps and polypropylene tubing. The tubing ended with a 18-gauge needle [18-g Becton Dickinson, Franklin Lakes, NJ] inserted into the rubber stopper. An additional needle inserted through the rubber stopper and connected to polypropylene tubing was used to pump out effluent from the reactors. A third needle was used to collect any biogas produced in the reactors. The rate of biogas production was measured with a respirometer [Challenge Environmental Systems, Cardiff, UK]. Inflow was provided from the top of the reactor and the outflow was collected from the bottom using longer needles for the outlet. All the equipment including tubing, needles, bottles, tubes was autoclaved prior to any reactor run. The reactors had 0.6 cm long stir bar inside and they were all placed on top of magnetic stirrers to allow for complete mixing (Figure 3.1).

For photosynthetic growth, the reactors were continuously illuminated by an incandescent light source (~10 W/m^2, as measured with a Yellow-Springs-Kettering model 6.5-A radiometer through a Corning 7-69 filter). The light was provided by five tubular incandescent light bulbs (940W, 130V, 440 lumens). The temperature was kept constantly at 30^oC by adjusting two external fans for proper heat dissipation. Figure 3.1 shows the overall experimental set-up for anaerobic photosynthetic experiments.

The aerobic chemostats had the same type of test tubes and connector tubing. However, the cultures were kept in dark and in a water bath with a constant temperature of 30^oC. Moreover, the inflow was provided from the bottom and the outflow was taken from the top as opposed to the

anaerobic set-up. Finally, aeration (2 mL/min from a compressed air cylinder) was provided by a long needle reaching to the bottom of the reactor, which also ensured complete mixing conditions for the aerobic chemostats without the need for stirring bars.

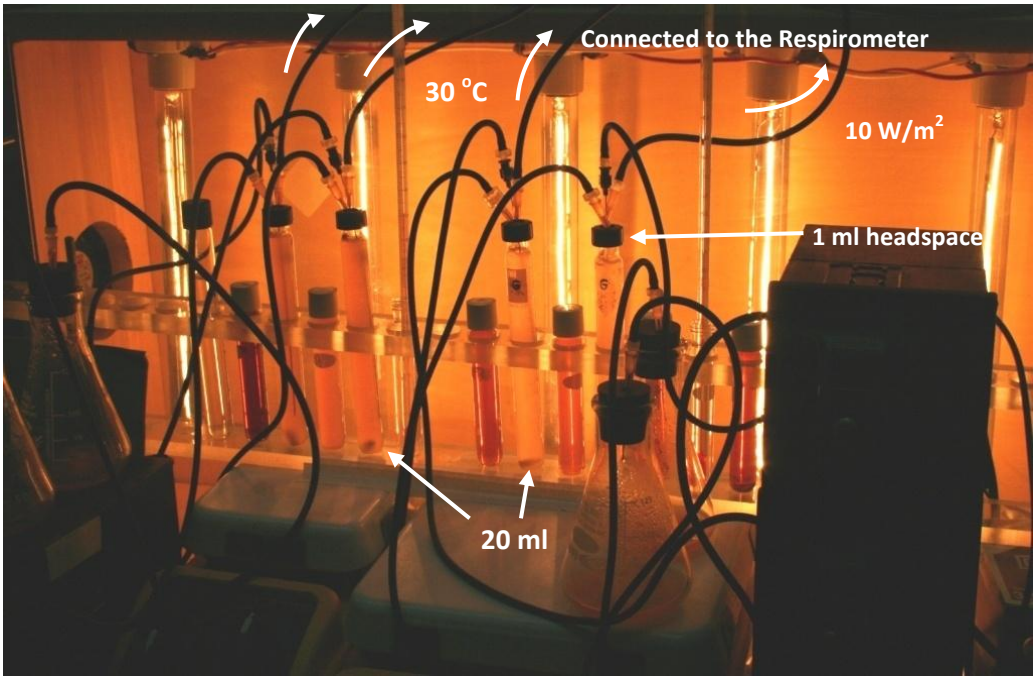

Figure 3.1 Anaerobic Chemostat Reactors Experimental Set-Up

Klett absorbance measurements were done with a Klett-Summerson photoelectric colorimeter [Klett MFG Co., NY] for determining cell growth. Near the end of experimental runs, Klett measurements were also taken multiple times in time intervals of a couple of hours to make sure that the culture reached steady-state conditions before sampling. In the case of aerobic chemostats, Optical Density (OD) (at 600 nm wavelength) measurements were done instead of Klett measurements for turbidity.

The targeted flow rates were calculated using the following formula:

$$\theta = \frac{V}{Q}$$

where θ is the hydraulic retention time, V is the active reactor volume (19 mL) and Q is the flow rate. Knowing the desired retention time and the active reactor volume, the flow rate was found and the pumps adjusted accordingly. Desired retention times were reached by pumping the liquid media continuously for 1 min in every 12 min (5 min pumping every hour). Cultures were grown for at least 5 retention times and stopped when steady state conditions were established as evidenced from constant Klett or OD readings as well as constant gas production rates.

3.2 SEED CULTURE CONDITIONS

Frozen glycerol stocks (15% glycerol) of WT *R. sphaeroides* 2.4.1 were used to inoculate the reactors. The origin of these stocks was anaerobic photosynthetic cultures grown on SIS medium with succinate as the carbon source and glutamic acid as the nitrogen source. The cultures were harvested when they reached a 0.9 OD reading.

3.3 MEDIA PREPARATION

Two different types of SIS Media were taken from the UW-Madison Bacteriology Department's Tim Donohue Laboratory: 10X Regular SIS with Succinate and Ammonia and 2X SIS without carbon source, with Glutamate as the nitrogen source. Briefly, 10X SIS media was diluted 10 times with Type I deionized water and then pH was adjusted to 7.0 using KOH pellets. The other media type which does not contain any carbon source was diluted 2 times with Type I deionized water and the desired carbon source was added, after which pH was again adjusted to 7.0 using KOH pellets. Different media were prepared with different carbon sources: Succinate, Glutamate, and Glucose as the carbon sources. As shown in

Table 3.1, the media had Glutamate or Ammonia as the nitrogen sources. All the media solutions were autoclaved (15 psi and 121^{o}C) for 30 minutes except for the medium with Glucose. Media that had Glucose was filter sterilized instead of autoclaved.

3.4 SAMPLE COLLECTION

As mentioned earlier, the samples were collected after reaching steady-state conditions, which was achieved after 3 to 6 days depending on the retention time of a specific chemostat. Prior to disconnecting the inflow, outflow and gas collection tubing, gas was sampled from the headspace and Klett measurements were taken. Sterile glass syringe [Hamilton, CO] was used with attached needle for puncturing the rubber septum. Gas was collected not only from the headspace of the reactor and but also from the tubing that was connected to the respirometer to allow for collecting approximately 4 mL of gas volume needed for analysis via Gas Chromatography (GC) (see section 4.1).

All the tubing was disconnected from the reactors by removing the needles from the rubber septum and final Klett measurements were taken. After that, the reactor was kept mixed as it was placed on top of a magnetic stirrer and 2 mL from the mixed culture was taken for the Chemical Oxygen Demand (COD) analysis. 12 mL of additional culture was transferred into pre-weighted sterile Pyrex glass vial for centrifugation (6000 rpm, 12 min, 4^{o}C), after which the supernatant was filtered through 0.2 µm sterile nylon syringe filter [Sartorius Ministart NY25, Edgewood, NY] into sterile 15 mL plastic centrifuge tubes [Corning, NY]. The cell pellet, the filtrate and the mixed whole culture were all stored at -80^{o}C before measuring the COD and analyzing the samples via GC-MS. The media used for each individual chemostat were also stored in the freezer for the same analyses described above. The details of these analyses are explained in Chapter 4.

CHAPTER 4 – EXPERIMENTAL PROCEDURES AND ANALYTICAL METHODS

4.1 REAL-TIME GAS PRODUCTION AND GC HEADSPACE COMPOSITION

The gas production in the photosynthetic cultures was monitored by a respirometer [Challenge Environmental Systems, Cardiff, UK] which was connected to a computer for recording the gas volume real time via its software [AER-ANR Version 1.02, Challenge Environmental Systems, Inc]. The data was then transferred to Excel for analyzing the gas production rates. The gas composition analysis was done via GC-2014 [Shimadzu Scientific, Columbia, MD]. The parameters are shown in Table 4.1.

Table 4.1 GC Details

Methanizer Temperature	380°C
Run Time	30 min
Column Maximum Temperature	60°C
Carrier Gas	Argon
Column Length	20 m
Column Thickness	0.5 µm
Column Diameter	0.32 mm
FID Detector	CO_2 and CO
FID Temperature	200°C
TCD Detector	H_2, N_2 and O_2
TCD Temperature	100°C
TCD Current	75 mA

4.2 CELL DRY WEIGHT

After each sampling the cell pellets were frozen inside the pre-weighted Pyrex glass vials which were lyophilized overnight with a VirTis 6K Benchtop lyophilizer [SP Industry, Gardiner, NY] at -60°C and 200 mtorr vacuum. The vials were then weighted and the difference between the weight of the original empty vial and the lyophilized sample corresponded to the cell dry weight. Using the cell dry weight, the biomass concentrations of the cultures at steady state and thus the growth rates could be calculated.

4.3 CHEMICAL OXYGEN DEMAND (COD) ANALYSIS

Establishing a COD Balance of the continuous *R. sphaeroides* cultures at steady state is needed for the development of its metabolic model and there are two approaches for determining the COD: experimental determination of COD and theoretical calculation of COD.

4.3.1 Experimental Determination of COD

Unfiltered culture COD and the filtered (soluble) COD was analyzed according to the AWWA Standard Method by using Hach COD Test Kit (high range; 0-1500 mg/L) (AWWA, 1999). This colorimetric method basically entails oxidation of all organic compounds in the sample by dichromate ($Cr_2O_7^{2-}$). The color change according to the amount of reacted dichromate indicates the oxidized organic matter concentration, thus the COD.

In order to determine the soluble COD of the cultures, the samples were first filtered through 0.2 µm sterile syringe filters [Millipore Millex ® GP, Bedford, MA] and then stored at -80^{o}C with the unfiltered cultures samples as explained in the previous chapter. All the samples were then thawed to room temperature and diluted 8 times. 2 mL of the samples (in duplicates) were added to the Hach COD vials for digestion on a Hach COD Reactor Heat Block [Hach Company, Loveland, CO] at 150 ^{o}C for 2 hours. After that the samples were allowed to cool down to room temperature and absorbance measurements at 600 nm were taken by a Spectronic ® Genesys Spectrophotometer [Milton Roy Company, USA]. Standard solution was prepared using potassium hydrogen phthalate (KPH) and Type I deionized water was used as the blank for absorbance measurements. As a quality control, new standard curve was prepared every time the samples analyzed and Figure 4.1 shows the average of the COD calibration curves.

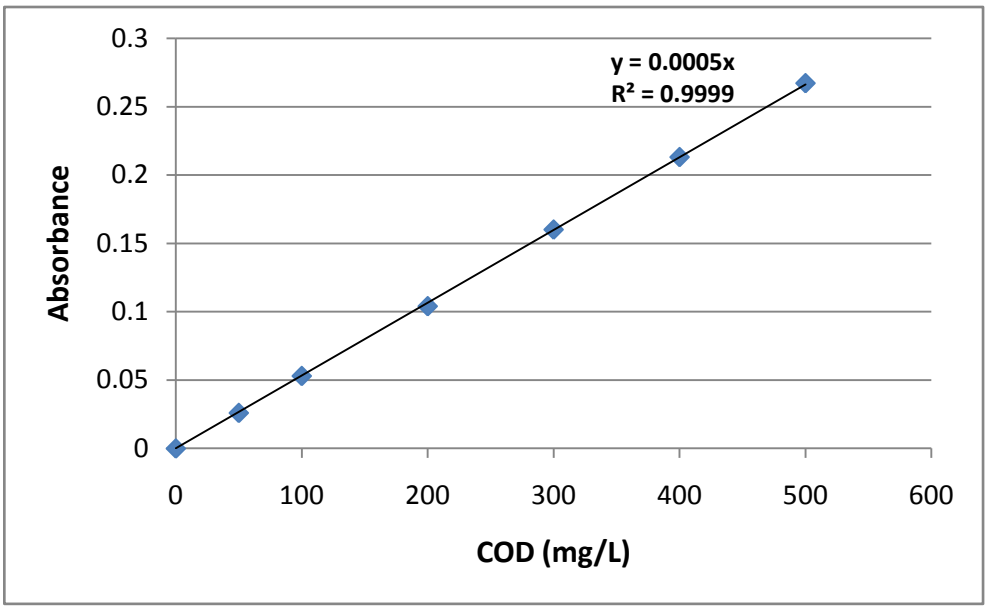

Figure 4.1 Average of five independent COD calibration curves. The standard deviation of the slope of the curve was $2*10^{-5}$

4.3.2 Theoretical Calculation of COD

The amount of nutrients in the media as well as in the cultures (carbon source and nitrogen source) are detected via GC-MS (see section 4.4.2) and quantified as molar concentrations. They are converted to theoretical COD concentrations (as mg/L) for creating a mass balance in terms of COD as explained in Section 2.4. For a compound that has the molecular designation of $C_nH_aO_bN_c$; the theoretical COD values are calculated according to the following equations (Ritmann et al., 2001):

$$\frac{COD'}{Weight} = \frac{16 * (2n + 0.5a - 1.5c - b)}{(12n + a + 16b + 14c)}$$

$$COD\ (mg/L) = \frac{COD'}{Weight} * MW * Conc.(M)$$

where *MW* is the molecular weight of the compound and *Conc.* is the molar concentration of the compound in the sample as quantified by the GC-MS.

4.4 MEASUREMENT OF THE COMPOUNDS

4.4.1 Liquid-liquid extraction: Methyl chloroformate derivatization

The method reported by Villas-Boas *et al.* (2003) was used for the analysis of the samples via GC-MS. The samples were derivatized with methyl chloroformate so that non-volatile metabolites in the samples could be converted to vaporizable derivatives and be detected via GC-MS by the methylation of organic and amino acids. In this study, succinate and glutamate were quantified via GC-MS.

The samples were first diluted so that the final concentrations would be within the range of 0-3 mM (the detection range via GC-MS). 1 mL of the samples (in duplicates) were transferred into Pyrex Glass vials and stored at -80^{o}C. The frozen samples were then lyophilized overnight. After lyophilization, 300 µL of 1% NaOH was added to the samples and mixed on Vortex Genie Mixer [Scientific Products; McGaw Park, IL] for 10 seconds. Then, 250 µL of absolute methanol and 50 µL pyridine was added respectively. Samples were again mixed on the vortex for 10 seconds. In order to ensure sufficient reaction time, samples were mixed 30 seconds after adding 30 µL of methyl chloroformate and the same step was repeated once more. The samples then received 600 µL of chloroform that contains Benzoic Acid Methyl Ester (BAME) as the internal standard (0.05% v/v) and vortexed again. Finally, as the last step before phase partitioning, 600 µL of 50 mM $NaHCO_3^-$ was added to the samples and mixed. The samples were allowed to wait at least 1 hour for phase partitioning.

After the aqueous phases partitioned, approximately 330 µL of the lower chloroform partition was transferred using ReachTips [Molecular BioProducts, San Diego] into GC vials with silanized glass vials inside. GC vials were then capped with micro-sert caps and septa for loading into the GC-MS machine for analysis.

4.4.2 Identification and Quantification via GC-MS

After the derivatization and phase partitioning, the samples were loaded into an automated Shimadzu Gas Chromatography-Mass Spectrometry (GC-MS) for analysis. The injection volume was 1 µL. The detailed instrument parameters can be found in Table 4.2. The instrument was connected to a computer that has the GCMS Solution Version 2.5 software [Shimadzu Scientific, Columbia, MD] for analysis of the compounds that are detected. Identifications of the peaks were done by 2007 National Institute of Standards and Technology (NIST) standard library. Succinate and glutamate had a retention time of 7.35 and 17.15 min, respectively. The standards were prepared for confirming the identification as well as the quantification (in terms of mM) of the identified peaks.

Table 4.2 GC-MS Instrument Parameters

Column Type	**SHRXI-5MS**
Column Oven Temperature	**60°C**
Carrier Gas	**He**
Column Length	**30 m**
Column Thickness	**0.25 µm**
Column Diameter	**0.25 mm**
Auto Injector Type	**AOC-201**
Injection Temperature	**180°C**
Injection Mode	**Split (1:5)**
MS Detector	**QP2010**
MS Detection Range	**35-500 m/z, 25 min**
Ion Source Temperature	**220°C**
Interface Temperature	**275°C**

4.4.3 Measurement of Glucose via HPLC

Glucose was quantified by High Performance Liquid Chromatography (HPLC) since it was not possible to detect sugars with methyl chloroformate derivatization. Table 4.3 shows the details of the HPLC sugar column. The operational settings were set according to the National Renewable Energy Laboratory. Diluted 1 mL of samples and standards were transferred to autosampler vials. The retention

time of glucose was 11.38 min and separation was achieved with BIORAD HPX-87P column, using 0.005 M H_2SO_4 as the mobile phase at a flow rate of 0.6 ml/min.

Table 4.3 HPLC sugar column and detector parameters

Sugar Detection Column Type	HPX-87P
Injection Volume	50 µL
Mobile Phase	0.005 M H_2SO_4
Flow Rate	0.6 mL/min
Column Temperature	80°C
Detector Temperature	80°C
Run Time	20 min
Detector	Refractive Index

CHAPTER 5 – RESULTS AND DISCUSSION

In this chapter, the results of five different experimental runs are shown as summarized earlier in Table 3.1 in Chapter 3. The first four experiments were conducted under anaerobic photosynthetic conditions, whereas the last one (Section 5.5) was conducted under aerobic dark conditions where oxygen was continuously supplied.

5.1 Succinate as the carbon source and Ammonia as the nitrogen source

The summary of the experimental data for the set of experiments conducted with the succinate as the carbon source and ammonia as the nitrogen source is shown in Table 5.1. With increasing retention times, slower specific growth rates were obtained and the electron partitioning for each different growth rate are tabulated in Table 5.2 and depicted in Figure 5.1 as ratios.

Table 5.1 Summary of key parameters at steady-state conditions

Retention Time	Klett Units	Biomass	Gas Rate	Specific Growth Rate
8 h	210	1200 mg/L	0.95 mL/h	0.125 h^{-1}
10 h	248	1300 mg/L	1.4 mL/h	0.1 h^{-1}
12 h	254	1400 mg/L	1.4 mL/h	0.083 h^{-1}
16 h	260	1400 mg/L	1.4 mL/h	0.063 h^{-1}

As expected, the biomass concentration increased with increasing retention times. However, gas production rate did not constantly increase as the growing cells move from exponential growth phase to stationary phase with slower specific growth rates.

Table 5.2 Summary of COD distribution per time at steady-state conditions

(mg COD/h)	Retention Times			
	8 h	**10 h**	**12 h**	**16 h**
Biomass COD	3.61	2.68	2.84	1.9
H_2 COD	0.52	0.77	0.77	0.77
SMP COD	0	1.26	1.63	1.34
COD Utilized	4.13	4.70	5.23	4.00
COD Utilized (Data from GC-MS)	3.59	4.45	4.11	3.58
Unknown	13%	5%	21%	11%

The values in Table 5.2 were obtained by multiplying the COD concentrations with the appropriate flow-rates to have a common unit of COD per hour because even though the biomass and SMP COD are originally found as mg/L at steady state conditions, the gas production rate is recorded as mL/hour. That is why it is important to do the proper conversions as described in previous chapters and analyze the data under the same units. "COD utilized" is basically the sum of biomass COD, H_2 COD and SMP COD since they all act as electron sinks, hence they represent the amount of electrons used up by the bacteria. The other "COD Utilized" data from the GC-MS represents the amount of carbon and nitrogen sources consumed by the organism in terms of COD units. Thus, in theory these two different values of COD utilized should be the same, however the difference is inevitable due to experimental errors and the possible other unknown electron sinks that consume COD at steady state conditions.

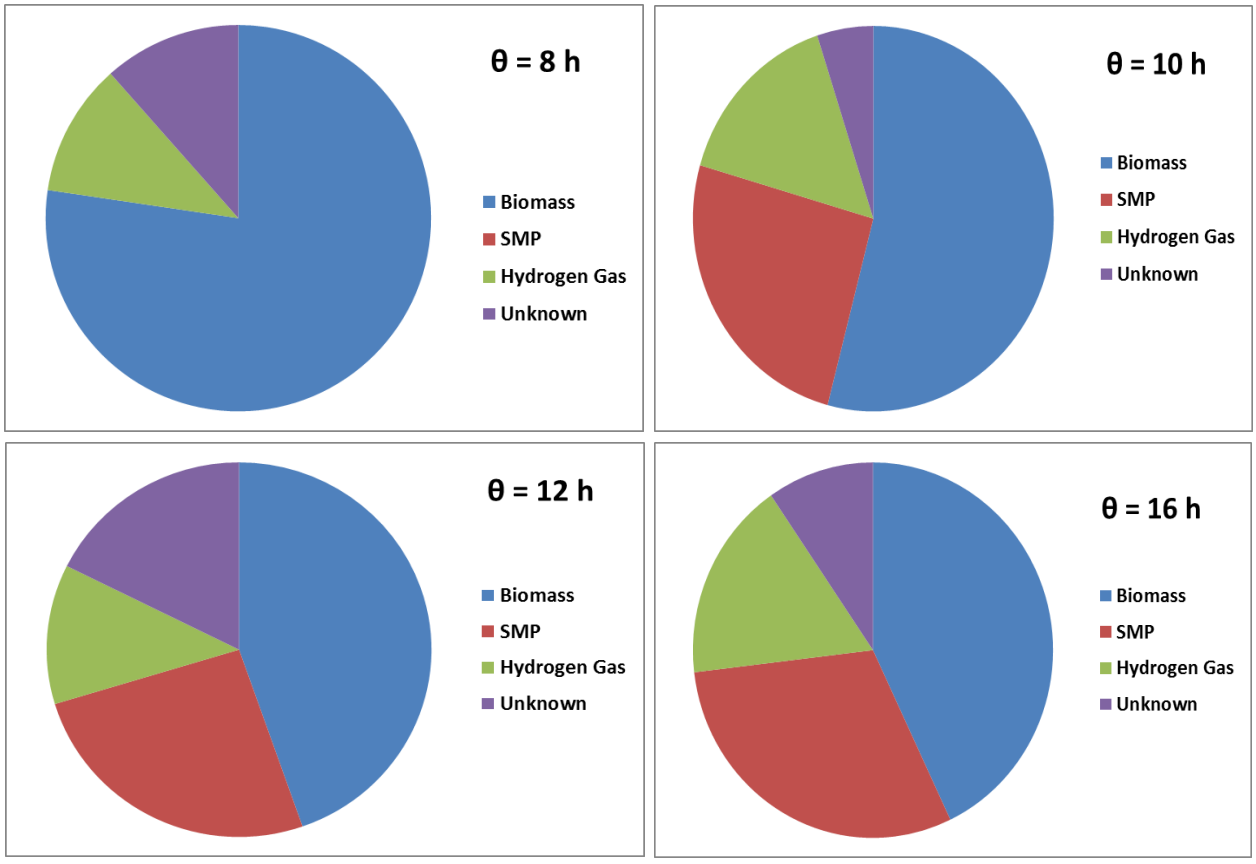

Figure 5.1 Electron partitioning with different retention times for the culture grown in Succinate and Ammonia.

As a result, the difference between these two COD values is designated as the unknown electron sinks other than the biomass, SMP and H_2 gas production. As can be seen from Figure 5.1, in general the major electron sinks appear to be the biomass and SMP. There is also significant H_2 gas production as the electron sink. The data from the culture with 8-h retention time shows no SMP and an overestimated biomass and it was not considered to be reliable, thus it was not included in the model. The specific growth rates do not seem to have any significant effect on the electron partitioning in these cultures.

5.2 Succinate as the carbon source and Glutamate as the nitrogen source

The same specific growth rates as the previous experimental set were achieved with the cultures that were fed succinate and glutamate as their carbon and nitrogen sources, respectively. The increase in the gas production rate was significant as the cells were forced to grow with lower specific growth rate and again as expected they had more biomass accumulation at steady state conditions with increasing retention times (Table 5.3). Quantitative electron partitioning values are shown in Table 5.4 and the relative ratios are depicted in Figure 5.2.

Table 5.3 Summary of key parameters at steady-state conditions

Retention Time	Klett Units	Biomass	Gas Rate	Specific Growth Rate
8 h	66	610 mg/L	0.7 mL/h	0.125 h^{-1}
10 h	150	870 mg/L	1.1 mL/h	0.1 h^{-1}
12 h	232	1360 mg/L	2.3 mL/h	0.083 h^{-1}
16 h	238	1470 mg/L	2.5 mL/h	0.063 h^{-1}

Table 5.4 Summary of COD distribution per time at steady-state conditions

(mg COD/h)	Retention Times			
	8 h	**10 h**	**12 h**	**16 h**
Biomass COD	0.56	1.71	2.77	1.89
H_2 COD	0.38	0.60	1.26	1.37
SMP COD	0	0	0.72	0.49
COD Utilized	0.94	2.31	4.75	3.74
COD Utilized (Data from GC-MS)	2.29	2.71	4.65	3.63
Unknown	59%	15%	2%	3%

Due to possible experimental errors in the analysis of carbon and nitrogen sources via GC-MS, there is a large portion of unknown electron sinks in the 8-h culture and again the data from 8-h culture was not included in the model. Another important point to mention is the lack of SMP as the electron sink in the 8-h and 10-h cultures contrary to the other experimental runs with different environmental and inflow media conditions. It is possible that the unknown portion of the electron pie chart could have some SMP but due to experimental errors with GC-MS, it could not have been detected. The most remarkable result of this experimental run was that the partitioning of substrate electrons into H_2 gas at 16 hour retention time was the highest among all the other conditions tested in this study.

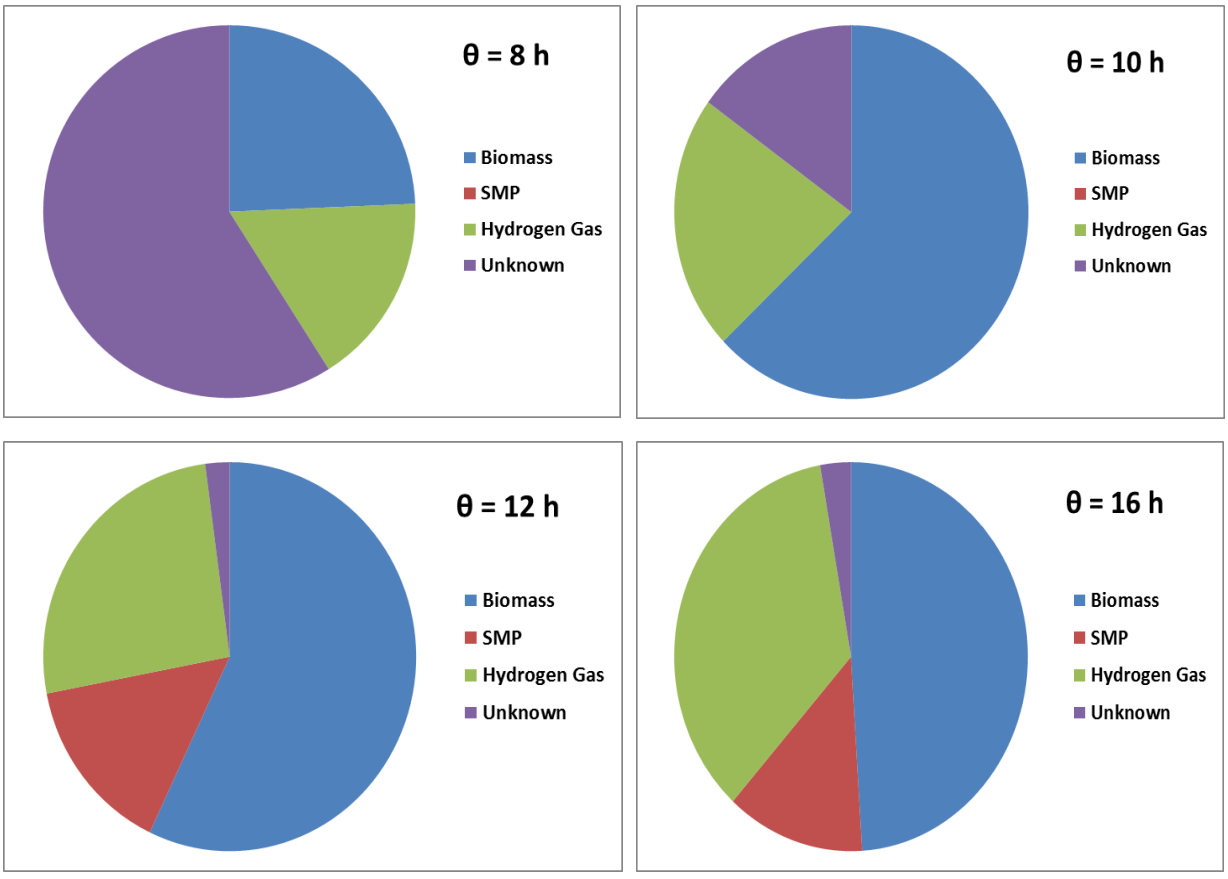

Figure 5.2 Electron partitioning with different retention times for the culture grown in Succinate and Glutamate.

5.3 Glutamate only as both the carbon source and the nitrogen source

Because *Rhodobacter* grows more slowly in the media that has only glutamate as the sole carbon and nitrogen source, the selection of retention times was slightly different from the previous experimental sets. Instead of starting with 8 hour retention time, the experimental set was started with a retention time of 10 hour and it was increased up to 24 hours (see Table 5.5 for summary). The amount of biomass production did not seem to be correlated with the specific growth rate as opposed to the cultures grown under different media conditions. Also, *Rhodobacter* did not produce any H_2 gas when fed with glutamate only, the large fraction of biomass in Figure 5.3 can be explained by the media type that was used since there was more nitrogen source that could allow more biomass production.

Table 5.5 Summary of key parameters at steady-state conditions

Retention Time	Klett Units	Biomass	Gas Rate	Specific Growth Rate
10 h	262	2200 mg/L	–	0.1 h^{-1}
12 h	264	2100 mg/L	–	0.083 h^{-1}
16 h	270	2000 mg/L	–	0.063 h^{-1}
24 h	274	2080 mg/L	–	0.042 h^{-1}

In general, in this case of growing *Rhodobacter* only in glutamate, at steady state conditions the majority of the substrate electrons were diverted into biomass production as well as some SMP production irrespective of the specific growth rate as shown in Figure 5.3 and Table 5.6.

Table 5.6 Summary of COD distribution per time at steady-state conditions

(mg COD/h)	Retention Times			
	10 h	**12 h**	**16 h**	**24 h**
Biomass COD	4.98	3.92	3.19	1.96
H_2 COD	0	0	0	0
SMP COD	0.82	0.71	0.55	0.39
COD Utilized	5.80	4.63	3.74	2.35
COD Utilized (Data from GC-MS)	5.93	4.95	3.71	2.47
Unknown	2%	6%	1%	5%

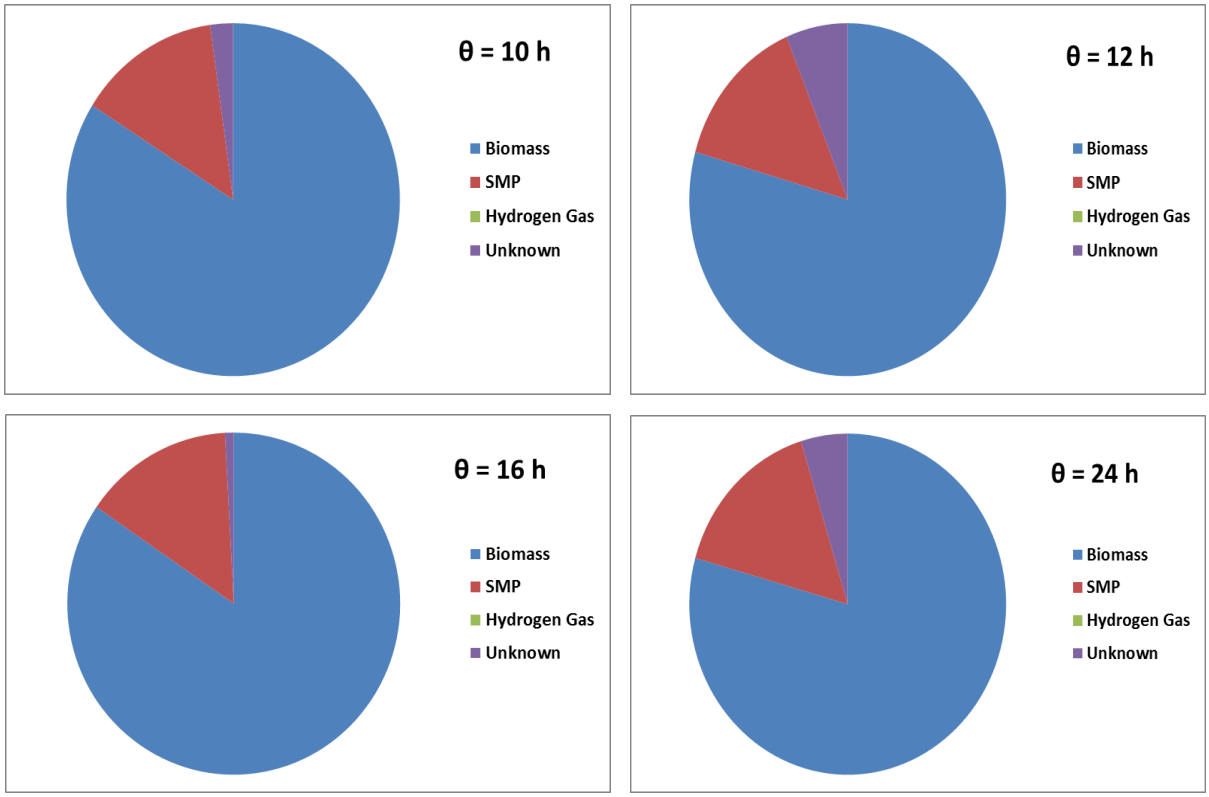

Figure 5.3 Electron partitioning with different retention times for the culture grown in Glutamate only.

5.4 Glucose as the carbon source and Glutamate as the nitrogen source

Rhodobacter was also grown in different specific growth rates in glucose in addition to the organic acids tested (Table 5.8 and Figure 5.4). Following the similar trends, there was increase in the gas production rate as well as in the production of biomass with a lower specific growth rate. In fact, the steady-state biomass production of the culture that had 12-hour retention time was the highest among all other conditions tested in this study, consistent with the previous findings that *Rhodobacter* produces the most biomass when it was fed glucose in batch cultures (Yilmaz et. al., 2010).

Table 5.7 Summary of key parameters at steady-state conditions

Retention Time	Klett Units	Biomass	Gas Rate	Specific Growth Rate
10 h	150	720 mg/L	0.68 mL/h	0.1 h^{-1}
12 h	184	950 mg/L	0.88 mL/h	0.083 h^{-1}

Table 5.8 Summary of COD distribution per time at steady-state conditions

(mg COD/h)	Retention Times	
	10 h	**12 h**
Biomass COD	1.52	2.22
H_2 COD	0.39	0.50
SMP COD	0.31	0.13
COD Utilized	2.22	2.84
COD Utilized (Data from GCMS and HPLC)	3.47	2.75
Unknown	36%	3%

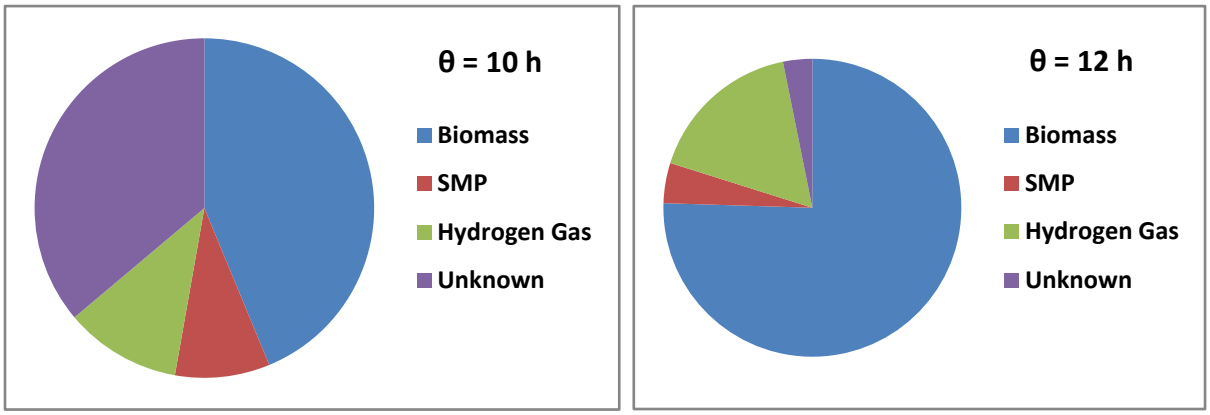

Figure 5.4 Electron partitioning with different retention times for the culture grown in Glucose and Glutamate.

5.5 Succinate as the carbon source and Ammonia as the nitrogen source under Aerobic Conditions

In the case aerobic growth, the key assumption was that the oxygen uptake rate corresponded to the difference between media COD and the COD of the culture at steady state (mixed COD) in order to have a complete mass balance. Thus, there was no unknown or error reported in the case of aerobic balance. While growing aerobically, O_2 consumption process (i.e. respiration) accounted almost half of the used substrate electrons (Figure 5.5). These results were used in flux balance analysis (FBA) of the model during aerobic respiratory growth on succinate and ammonia under different specific growth rates (Saheed et. al., submitted).

Table 5.9 Summary of key parameters at steady-state conditions

Retention Time	Klett Units	Biomass	Gas Rate	Specific Growth Rate
7.1 h	190	340 mg/L	–	0.141 h^{-1}
8.7 h	170	340 mg/L	–	0.115 h^{-1}
9.3 h	165	340 mg/L	–	0.108 h^{-1}
9.5 h	105	340 mg/L	–	0.105 h^{-1}

Table 5.10 Summary of COD distribution per time at steady-state conditions

COD (mg/L)	Retention Times			
	7.1 h	8.7 h	9.3 h	9.5 h
Media COD	2891	3027	2987	2827
Soluble COD	1507	1339	1571	1667
Mixed COD (Whole culture)	2131	2091	2139	2187
Biomass COD	624	752	568	520
SMP COD	225	65	409	72
COD Uptake (O_2 Respiration)	760	936	848	640

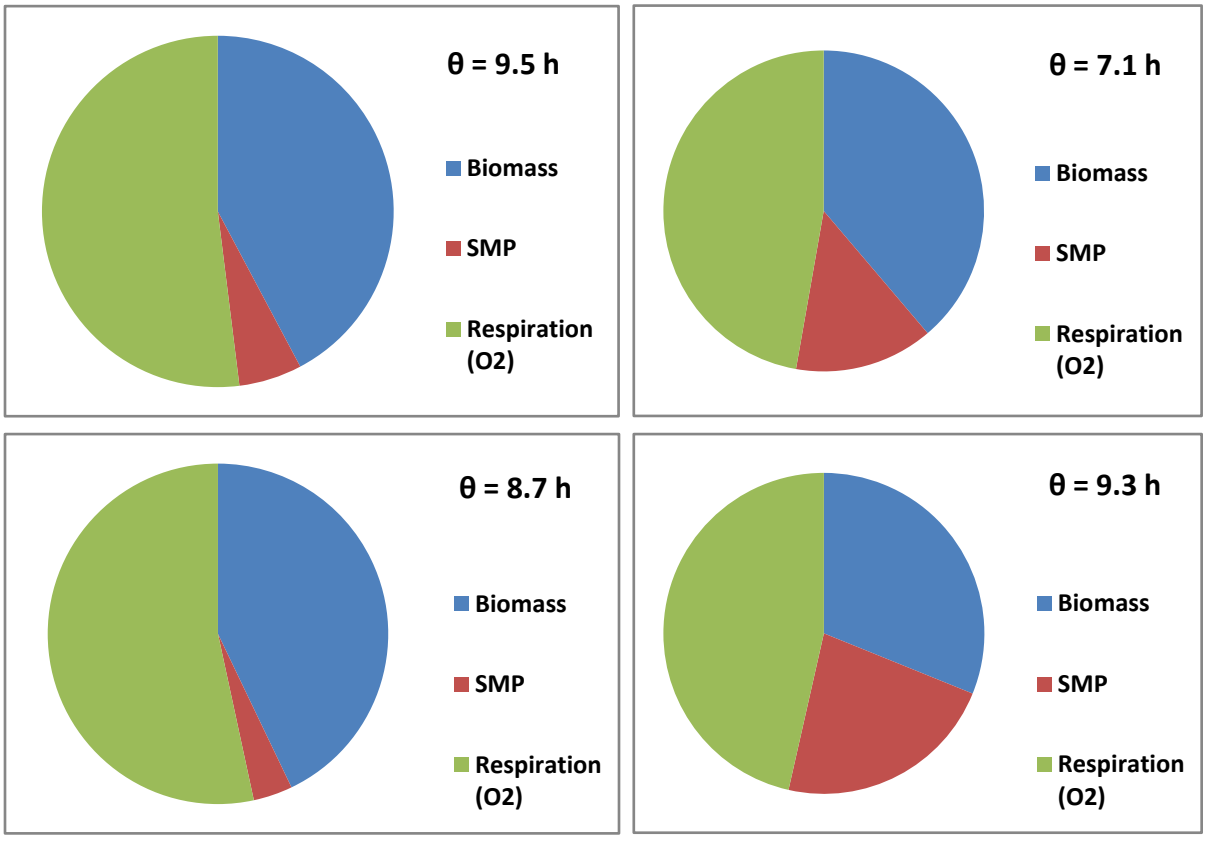

Figure 5.5 Electron partitioning during aerobic growth for the culture grown in Glucose and Ammonia.

CHAPTER 6 – CONCLUSIONS AND RECOMMENDATIONS

This study investigated the electron partitioning of reducing power in different lifestyles of continuous *R. sphaeroides* cultures. In addition to being a facultative bacterium capable of living under different environmental conditions, *R. sphaeroides* has received significant attention due to its biotechnological potential with its ability to produce large amounts of H_2 gas and fatty acids as potential biofuels.

Here it was shown the optimum conditions in terms of maximizing the potential biofuel production in continuous cultures. For instance, if the goal is to produce H_2 gas as the biofuel, then industrial wastes containing organic acids such as succinic acid can be used for feeding the bacteria at longer retention times, in other words, the bacterium should be forced to have lower specific growth rate to maximize H_2 production. However, if the goal is to produce biodiesel from the accumulation of fatty acids of *R. sphaeroides,* then a glucose rich medium such as renewable cellulosic material can be used to maximize the biomass (hence the fatty acid) production.

Metabolic modeling of this bacterium by using experimental data of this study will increase the understanding of its versatile and complex pathways. This will eventually allow engineering its metabolism to divert substrate reducing power to biofuel production. While the fate of substrate electrons have previously been studied quantitatively in batch cultures for understanding the major metabolic pathways (Yilmaz et. al., 2010), the electron partitioning data from continuous cultures under diverse environmental conditions (such as dark aerobic, photosynthetic H_2 producing and photosynthetic non-H_2 producing conditions) was needed for the quantitative assessment of the metabolic network model of *R. sphaeroides*. Named as iRsp1095, this manually curated genome-scale metabolic reconstruction for *R. sphaeroides* was recently evaluated for the H_2 production potential of this bacterium (Saheed et. al., submitted). Hence this study has contributed to the more detailed analyses of

this organism via development of its metabolic network model to determine metabolic limitations and to design genetic approaches to maximize biofuel production. Further experimental work would be helpful to confirm the quantitative model predictions leading to an improved understanding of photosynthetic microorganisms which can be harnessed for the benefit of the planet and society in terms of harvesting solar energy and sequestering atmospheric carbon dioxide.

REFERENCES

AWWA. (1999) *Standard Methods for the Examination of Water & Wastewater.* Washington, D.C: American Public Health Association, American Water Works Association, Water Pollution Control Federation (APHA-AWWA-WPCF)

Baptiste J. P., Ducroux R., (2003) Energy Policy and Climate Change. *Energy Policy* **31**:155-166

Demirbas A., (2007) Progress and recent trends in biofuels. *Progress in Energy and Combustion Science* **33**:1-18

Herbert D. (1958) In *Recent Progress in Microbiology, VII International Congress for Microbiology,* ed. Tunevall G., p. 381. Almquist & Wiksell, Stockholm

Kapdan I. K., Kargi F., (2006) Biohydrogen production from waste materials. *Enzyme and Microbial Technology* **38**: 569-582

Levin D. B., Pitt L., Love M., (2004) Biohydrogen production: prospects and limitations to practical application. *International journal of Hydrogen Energy* **29**: 173-185

Marban G., Solis T. V., (2007) Towards the hydrogen economy? *International Journal of Hydrogen Energy* **32**: 1625-1637

Monod J. (1950) *Ann. Inst. Pasteur.,* **79**: 390-410

Pirt, S. J. (1975) *Principles of Microbe and Cell Cultivation*. Blackwell Scientific Publications

Rittman, B. & McCarty, PL. (2001) *Environmental Biotechnology: Principles and Applications.* McGraw-Hill

Saheed Imam, L. Safak Yilmaz, Ugur Sohmen, Alex Gorzalski, Jennifer L. Reed, Daniel R. Noguera, and Timothy J. Donohue. iRsp1095: A Genome-scale Reconstruction of the *Rhodobacter sphaeroides* metabolic network (submitted to *Genome Biology*)

Villas-Boas, S. G., Delicado, D. G., Akesson, M., and Nielsen, J. (2003) Simultaneous analysis of amino and nonamino organic acids as methyl chloroformate derivatives using gas chromatography – mass spectrometry. *Mass Spectrometry Reviews* **24:**613-646

Yilmaz LS, Kontur, W. S., Sanders, A. P., Sohmen, U., Donohue, T. J. and D. R. Noguera (2010) Electron partitioning during light- and nutrient-powered hydrogen production by *Rhodobacter sphaeroides Bioenerg Research*, **1**:55 - 66.